IMEKO, IEEE, SICE
2nd International Symposium on Measurement, Analysis and Modeling of Human Functions
1st Mediterranean Conference on Measurement
June 14-16, 2004, Genova, Italy

IMPEDANCE SIMULATOR: ANALYSIS OF HUMAN HAND IMPEDANCE CHARACTERISTICS

Yusaku Takeda, Yoshiyuki Tanaka, and Toshio Tsuji

Department of Artificial Complex Systems Engineering, Hiroshima University
Higashi-Hiroshima, 739-8527 JAPAN

1. INTRODUCTION

A human performs a variety of skillful motions by adjusting dynamic characteristics of his/her musculoskeletal system in motion. Therefore, when considering the use of robots which would be in direct interaction with humans, it is necessary to design the whole system with full consideration of the human movement system.

Generally, human movements have been often described with mechanical impedance parameters; i.e., stiffness, viscosity, and inertia. Many experimental studies on human arm impedance have been reported. For example, Mussa-Ivaldi et al. [1] pioneered the measurement of human hand impedance, and examined hand stiffness in a stable arm posture. It was reported that hand stiffness depends greatly on a arm posture and that a human can change the magnitude of stiffness at will but not its direction. Dolan et al. [2] and Tsuji et al. [3] investigated not only hand stiffness but also viscosity and inertia, and verified a qualitative analogy between hand stiffness and viscosity. Also, Tsuji et al. [4],[5] found that the hand viscoelastic characteristics change in proportion to the muscle contraction level. Furthermore, Tsuji et al. [4],[5], Osu and Gomi [6] attempted to estimate human joint impedance parameters in dynamic motion from the EMG signals. Gomi et al. [7] then examined hand impedance in reaching movements and demonstrated that hand stiffness in motion changes activity more than one in a stable arm posture.

As opposed to the above experimental studies, some reports attempted to reveal mentioned voluntary arm movements and the motor control mechanism using computer simulations. Flash [8] performed computer simulations of a two-joint planar arm based on the virtual trajectory control hypothesis. She showed that simulated results using straight virtual trajectories determined by a minimum jerk criterion found measured trajectories of the human arm and computer simulations to be nealy alike. Also, Katayama and Kawato [9] proposed a parallel hierarchical neural network model which includes inverse static and dynamics models. The inverse static model mainly controls the equilibrium posture and the human joint stiffness, and the inverse dynamics model plays a role in compensating the non-linear dynamics of the arm during fast movements. They found through computer simulations using a two-joint, six-muscle arm model that the virtual trajectories learned during fast movements largely differed from the actual arm trajectories. However, in computer simulations of two-joint arms, for example, different values of the viscoelastic coefficients of joints or muscles may determine quite different simulation results. In order to validate the mechanism of voluntary arm movements, it is necessary to rely on precise estimates of the viscoelastic property according to the change of the arm posture and muscle contraction levels.

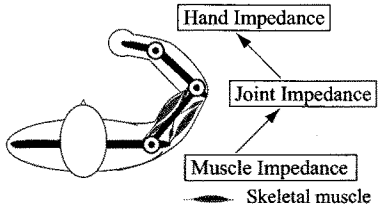

Fig. 1. Explanation of impedance transfer.

However, it may not be expected to measure hand impedance in motion accurately because hand impedance is influenced significantly by the conditions of the musculoskeletal system which varies by the contraction intensity, the arrangement of various muscles, and the sensitivity of the spinal reflex. Besides, it may be difficult to measure the hand impedance with maintained posture depending on environmental conditions and immeasurable postures. If the hand impedance was predicted under any condition, we could reveal the characteristic of human upper extremities without measuring the hand impedance.

The goal of this study is to develop an *impedance simulator*, which can predict hand impedance according to the configurations of upper extremities and joint activation levels by using measured hand impedance data [3]–[5]. Validity of the developed simulator is evaluated through comparison with the estimated impedance of a single arm.

2. REGULATION MECHANISM OF HUMAN MECHANICAL IMPEDANCE

The human body mainly has two impedance regulation mechanisms; i.e., the variable dynamic characteristics of

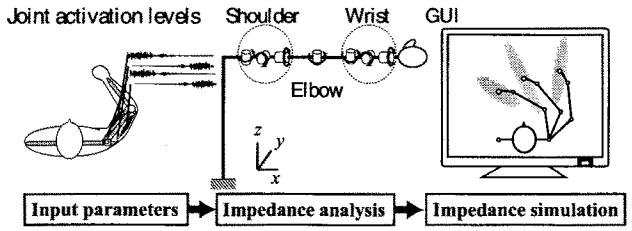

Fig. 2. Impedance simulation.

skeletal muscles, and the redundant structure of a musculoskeletal system.

A skeletal muscle has the characteristics not only of a force actuator but also of a variable viscoelastic component according to the motor command from the central nervous system. Also, in Fig. 1, the muscle impedance is transferred to a hand through the dynamic structure of the skeletal system, and serves as a generation source of the hand impedance.

Therefore, if a muscle has been stiffened, the motion of the hand also becomes stiff, and vice versa. Also, if the arm posture has been changed, the hand impedance characteristics are changed as a result of modifying the transfer characteristics from muscles to the hand. It means that hand impedance can be adjusted by regulating the joint angle of the shoulder, elbow and wrist, as shown in Fig. 1.

In this paper, we constructed an *impedance simulator* for predicting the mechanical impedance characteristics of the human body based on arm postures and joint activation levels.

3. IMPEDANCE SIMULATOR

3.1. System structure

Figure 2 depicts a process of simulating the hand impedance, in which a musculoskeletal system of a human arm is modeled by a 7 DOF multi-joint link with 3 links: shoulder and wrist joints are modeled by ball joints with three DOFs and elbow joints a pin joint with one DOF. The developed simulator has a database of hand impedance parameters measured by Tsuji et al. [3]–[5], and can predict hand impedance characteristics according to posture and joint activation levels. Computed results are showed by 3D computer graphics in the display. Next, the method to compute the hand impedance in upper extremities is explained.

3.2. Impedance in multi-joint arms

In the part of impedance analysis in Fig. 2, the hand impedance is simulated based on kinematics and dynamics of multi-joint arms. The position vectors in the joint coordinates and end-point coordinates are denoted as $\boldsymbol{q} \in \Re^7$ and $\boldsymbol{X} \in \Re^2$, respectively. Where the generalized force vectors in the joint coordinates and end-point coordinates are denoted $\boldsymbol{\tau} \in \Re^7$ and $\boldsymbol{F} \in \Re^2$, respectively, we can have

$$\boldsymbol{\tau} = \boldsymbol{J}(\boldsymbol{q})^T \boldsymbol{F}, \tag{1}$$

where $\boldsymbol{J}(\boldsymbol{q}) \in \Re^{2\times 7}$ is the Jacobian matrix.

On the other hand, a hand impedance model can be expressed in the end-point level when the human arm is under a stable posture:

$$\boldsymbol{M}_e\ddot{\boldsymbol{X}} + \boldsymbol{B}_e\dot{\boldsymbol{X}} + \boldsymbol{K}_e(\boldsymbol{X} - \boldsymbol{X}_v) = \boldsymbol{F} + \boldsymbol{F}_{ext}, \tag{2}$$

where $\boldsymbol{M}_e, \boldsymbol{B}_e, \boldsymbol{K}_e \in \Re^{2\times 2}$ represent the hand inertia, viscosity, stiffness matrices, respectively. $\boldsymbol{X}_v$ represents the virtual equilibrium point, and $\boldsymbol{F}_{ext}$ the external force. A corresponding joint impedance model is assumed in the joint level:

$$\boldsymbol{M}_q\ddot{\boldsymbol{q}} + \boldsymbol{B}_q\dot{\boldsymbol{q}} + \boldsymbol{K}_q(\boldsymbol{q} - \boldsymbol{q}_v) = \boldsymbol{\tau} + \boldsymbol{\tau}_{ext}, \tag{3}$$

where $\boldsymbol{M}_q, \boldsymbol{B}_q, \boldsymbol{K}_q \in \Re^{7\times 7}$ represent the joint inertia, viscosity, stiffness matrices, respectively. $\boldsymbol{q}_v$ represents the virtual equilibrium point in the joint level, and $\boldsymbol{\tau}_{ext}$ the external joint torque which is generated by $\boldsymbol{F}_{ext}$. Then, the impedance relationships between joint and end-point levels can be derived using Eqs.(1)~(3) as follows [10]:

$$\boldsymbol{M}_q = \boldsymbol{J}(\boldsymbol{q})^T \boldsymbol{M}_e \boldsymbol{J}(\boldsymbol{q}), \tag{4}$$

$$\boldsymbol{B}_q = \boldsymbol{J}(\boldsymbol{q})^T \boldsymbol{B}_e \boldsymbol{J}(\boldsymbol{q}), \tag{5}$$

$$\boldsymbol{K}_q = \boldsymbol{J}(\boldsymbol{q})^T \boldsymbol{K}_e \boldsymbol{J}(\boldsymbol{q}) + \frac{\partial \boldsymbol{J}(\boldsymbol{q})}{\partial \boldsymbol{q}} \boldsymbol{F}_{ext}, \tag{6}$$

The hand impedance characteristics change according to the posture of the upper extremities and the muscle activation levels [3]–[5]. Therefore, we newly define the joint activation levels $\boldsymbol{\alpha} = \mathrm{diag.}(\boldsymbol{\alpha}_s^T, \boldsymbol{\alpha}_e^T, \boldsymbol{\alpha}_w^T)$, which is grouped activation levels of muscles that operate upon the shoulder, elbow and wrist joints. The activation vectors of joints are denoted as $\boldsymbol{\alpha}_s \in \Re^3$, $\boldsymbol{\alpha}_e \in \Re^1$, $\boldsymbol{\alpha}_w \in \Re^3$, respectively.

Then, joint impedance matrix $\boldsymbol{A}_q(\boldsymbol{\alpha}, \boldsymbol{q}) \in \Re^{7\times 7}$ ($\boldsymbol{A}_q \in \{\boldsymbol{M}_q, \boldsymbol{B}_q, \boldsymbol{K}_q\}$) is represented by the vector $\boldsymbol{\alpha}$ as follows:

$$\boldsymbol{A}_q(\boldsymbol{\alpha}, \boldsymbol{q}) = \boldsymbol{\alpha}^{\frac{1}{2}} \widetilde{\boldsymbol{A}}_q(\boldsymbol{q}) \boldsymbol{\alpha}^{\frac{1}{2}}, \tag{7}$$

where $\boldsymbol{\alpha}^{\frac{1}{2}}$ denotes the diagonal matrix, which has elements of square root of $\boldsymbol{\alpha}$. Note that $\boldsymbol{\alpha}$ is replaced by the identify matrix for the inertia $\boldsymbol{M}_q$. Then, $\widetilde{\boldsymbol{A}}_q(\boldsymbol{q})$ can be defined as

$$\widetilde{\boldsymbol{A}}_q(\boldsymbol{q}) = \begin{bmatrix} \widetilde{\boldsymbol{A}}_{ss}(\boldsymbol{q}) & \widetilde{\boldsymbol{A}}_{se}(\boldsymbol{q}) & \widetilde{\boldsymbol{A}}_{sw}(\boldsymbol{q}) \\ \widetilde{\boldsymbol{A}}_{se}^T(\boldsymbol{q}) & \widetilde{\boldsymbol{A}}_{ee}(\boldsymbol{q}) & \widetilde{\boldsymbol{A}}_{ew}(\boldsymbol{q}) \\ \widetilde{\boldsymbol{A}}_{sw}^T(\boldsymbol{q}) & \widetilde{\boldsymbol{A}}_{ew}^T(\boldsymbol{q}) & \widetilde{\boldsymbol{A}}_{ww}(\boldsymbol{q}) \end{bmatrix}, \tag{8}$$

where $\widetilde{\boldsymbol{A}}_{ss}(\boldsymbol{q}) \in \Re^{3\times 3}$, $\widetilde{\boldsymbol{A}}_{ee}(\boldsymbol{q}) \in \Re^1$ and $\widetilde{\boldsymbol{A}}_{ww}(\boldsymbol{q}) \in \Re^{3\times 3}$ represent the joint impedance matrices of the shoulder, elbow and wrist joints, respectively. Also, $\widetilde{\boldsymbol{A}}_{se}(\boldsymbol{q}) \in \Re^{3\times 1}$, $\widetilde{\boldsymbol{A}}_{sw}(\boldsymbol{q}) \in \Re^{3\times 3}$ and $\widetilde{\boldsymbol{A}}_{ew}(\boldsymbol{q}) \in \Re^{1\times 3}$ represent the interaction terms between the shoulder and elbow joints, the shoulder and wrist joints, the elbow and wrist joints, respectively. The relationships between the hand impedance matrix $\boldsymbol{A}_e(\boldsymbol{\alpha}, \boldsymbol{q}) \in \Re^{2\times 2}$ ($\boldsymbol{A}_e \in \{\boldsymbol{M}_e, \boldsymbol{B}_e, \boldsymbol{K}_e\}$) and the joint impedance matrix $\widetilde{\boldsymbol{A}}_q(\boldsymbol{q}) \in \Re^{7\times 7}$ ($\widetilde{\boldsymbol{A}}_q \in \{\boldsymbol{M}_q, \boldsymbol{B}_q, \boldsymbol{K}_q\}$) can be represented as follows:

$$\boldsymbol{A}_e(\boldsymbol{\alpha}, \boldsymbol{q}) = \left\{ \boldsymbol{J}(\boldsymbol{q}) \boldsymbol{\alpha}^{-\frac{1}{2}} \widetilde{\boldsymbol{A}}_q^{\sharp}(\boldsymbol{q}) \boldsymbol{\alpha}^{-\frac{1}{2}} \boldsymbol{J}^T(\boldsymbol{q}) \right\}^{-1} \tag{9}$$

where $()^{\sharp}$ represent the pseudo-inverse matrix.

In this paper, we constructed an *impedance simulator* based on Eqs.(4)~(9).

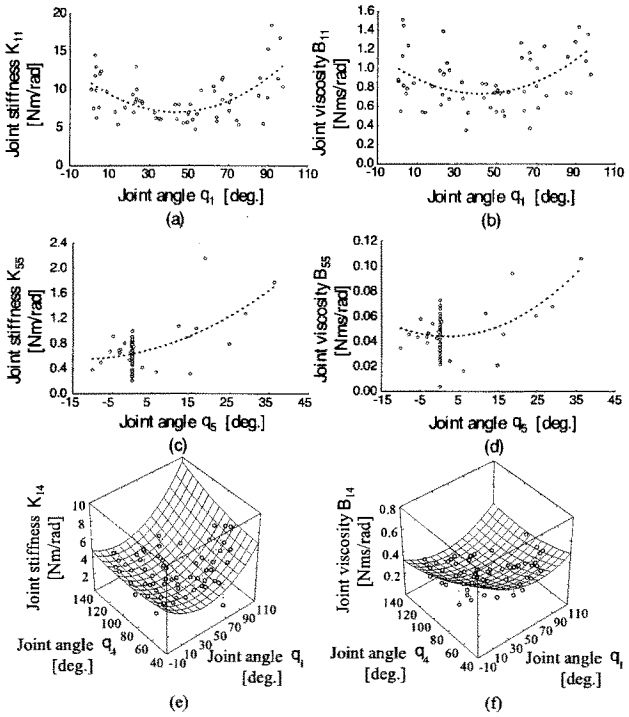

Fig. 3. Example of the approximated diagonal elements and interaction terms of joint stiffness and viscosity matrices with respects to joint angles.

3.3. The simulation method

First, the joint impedance matrix $\boldsymbol{A}_q(\boldsymbol{q}^l)$ $(l = 1, \cdots, n)$ has been simulated by the measured hand impedance matrices in a certain arm posture $\boldsymbol{q}^l$ [3]–[5]. Next, the joint impedance matrix $\boldsymbol{A}_q(\boldsymbol{q})$ has been modeled by the polynomial approximation using other subject's elements of joint impedance parameters $\boldsymbol{A}_q(\boldsymbol{q}^l)$ measured on various locations [3].

Weiss et al. [11] showed the ankle joint stiffness and viscosity parameters were small around the mid-range of the motion range and increased by extension and flexion of the ankle joint. The ankle joint inertia was essentially constant throughout the range of motion. Therefore, the relationship between joint viscoelasticity and the joint angle is modeled by the second order polynomial approximation, and the relationship between the joint inertia and the joint angle is modeled by the first order polynomial approximation. For example, the relationship between the joint stiffness and the joint angle can be represented as follows:

$$\widetilde{K}_{q_{ii}} = b_1^{ii} + a_1^{ii} q_i + a_2^{ii} (q_i)^2, \tag{10}$$

$$\widetilde{K}_{q_{ij}} = b_2^{ij} + a_3^{ij} q_i + a_4^{ij} q_j + a_5^{ij} (q_i)^2 + a_6^{ij} q_i q_j + a_7^{ij} (q_j)^2, \tag{11}$$

where b_1^{ij}, b_2^{ij} and a_m^{ij} $(i,\ j,\ m = 1, 2, \cdots, 7)$ are coefficients for modeling the joint stiffness. These coefficients included in the polynomials were estimated by the standard least square method. q_1, q_2, $\cdots$, q_7 represent a joint angle of the shoulder flexion and extension, the shoulder adduction and abduction, the shoulder internal rotation and external rotation, the elbow flexion and extension, the wrist flexion and extension, the wrist pronation and supination, and the wrist radial deviation and ulnar deviation, respectively. The origins of each joint angle 0 [deg.] are the posture which lengthened the arm on the right, and the arrows indicate the positive rotational directions in Fig. 2. Substituting Eqs.(10)~(11) into Eq.(8) yields the joint stiffness. Thus, the joint viscosity and inertia can be modeled by the same way as the modeling method of joint stiffness. On the other hand, Tsuji et al. [4],[5] showed that elements of joint stiffness and viscosity matrices can be represented using the linear summation of muscle activation levels. Therefore, this study assumes that the joint stiffness and viscosity increase in proportion to joint activation levels.

Then, the hand impedance of a single arm can be simulated according to the arm posture $\boldsymbol{q}$ and joint activation level α from Eq.(9). Hereafter, the simulated value is called the simulated hand impedance, and the measured value is called the measured hand impedance.

TABLE I

EXAMPLE OF COEFFICIENTS IN THE POLYNOMIAL APPROXIMATING THE JOINT STIFFNESS.

(a) Coefficients of the elements of joint stiffness matrix $\widetilde{K}_{q_{ii}}(q_i)$.

	b_1^{ii}	a_1^{ii}	a_2^{ii} ($\times 10^{-4}$)
$\widetilde{K}_{q_{11}}(q_1)$	10.932	-0.180	20.000
$\widetilde{K}_{q_{55}}(q_5)$	0.635	0.013	4.696

(b) Coefficients of the elements of joint stiffness matrix $\widetilde{K}_{q_{ij}}(q_i, q_j)$.

	b_2^{ij}	a_3^{ij}	a_4^{ij}	a_5^{ij} ($\times 10^{-4}$)	a_6^{ij} ($\times 10^{-4}$)	a_7^{ij} ($\times 10^{-4}$)
$\widetilde{K}_{q_{14}}(q_1, q_4)$	5.517	-0.074	-0.04	7.795	2.509	2.222

TABLE II

EXAMPLE OF COEFFICIENTS IN THE POLYNOMIAL APPROXIMATING THE JOINT VISCOSITY.

(a) Coefficients of the elements of joint stiffness matrix $\widetilde{B}_{q_{ii}}(q_i)$.

	b_1^{ii}	a_1^{ii} ($\times 10^{-4}$)	a_2^{ii} ($\times 10^{-5}$)
$\widetilde{B}_{q_{11}}(q_1)$	1.005	-130.000	15.460
$\widetilde{B}_{q_{55}}(q_5)$	0.044	-1.735	4.608

(b) Coefficients of the elements of joint stiffness matrix $\widetilde{B}_{q_{ij}}(q_i, q_j)$.

	b_2^{ij}	a_3^{ij}	a_4^{ij}	a_5^{ij} ($\times 10^{-4}$)	a_6^{ij} ($\times 10^{-4}$)	a_7^{ij} ($\times 10^{-4}$)
$\widetilde{B}_{q_{14}}(q_1, q_4)$	0.874	-0.007	-0.008	0.437	0.237	0.250

3.4. The simulation results

Figure 3 shows the examples of the measured diagonal elements of the joint stiffness and viscosity matrices as the white circles, according to the right arm posture. The predicted element values of the joint stiffness and viscosity matrices using the second order polynomial models are represented as the 2D broken lines and 3D surfaces. Figures 3(a) and (b) show joint stiffness and viscosity in shoulder flexion and extension within 0.47 ~ 97.47 [deg.] , Figs. 3(c) and (d) show joint stiffness and viscosity in wrist flexion and extension within -10.07 ~ 36.22 [deg.] , and Figs. 3(e) and (f) show interaction terms of the joint stiffness and viscosity between the shoulder and elbow in shoulder flexion and extension within 0.47 ~ 97.47 [deg.], and elbow flexion and extension within 47.88 ~ 129.59 [deg.]. Tables I and II show examples of coefficients in these polynomials approximating the joint stiffness and viscosity in Fig. 3. The hand impedance was

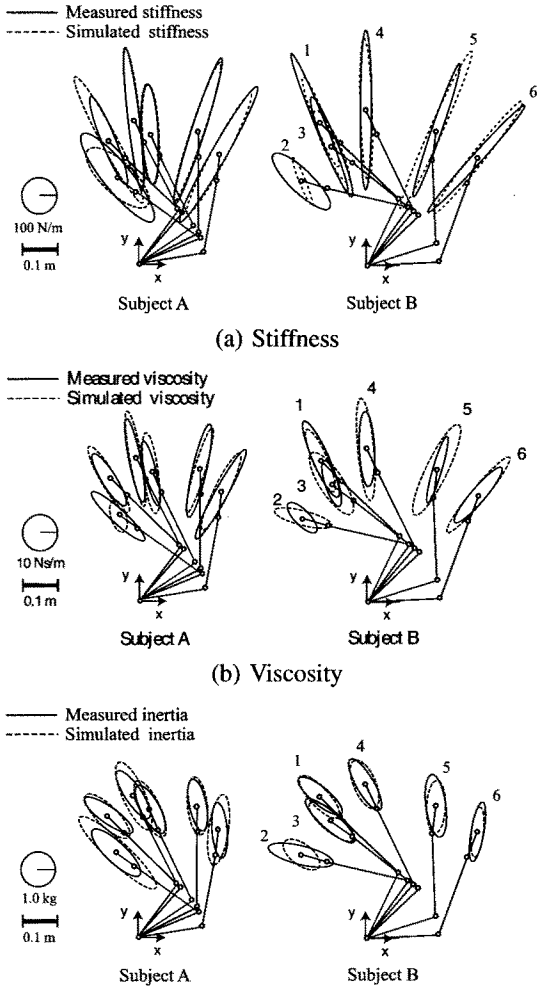

Fig. 4. Comparison between measured and simulated impedance ellipses of the single arm with changing 2D arm posture for two subjects.

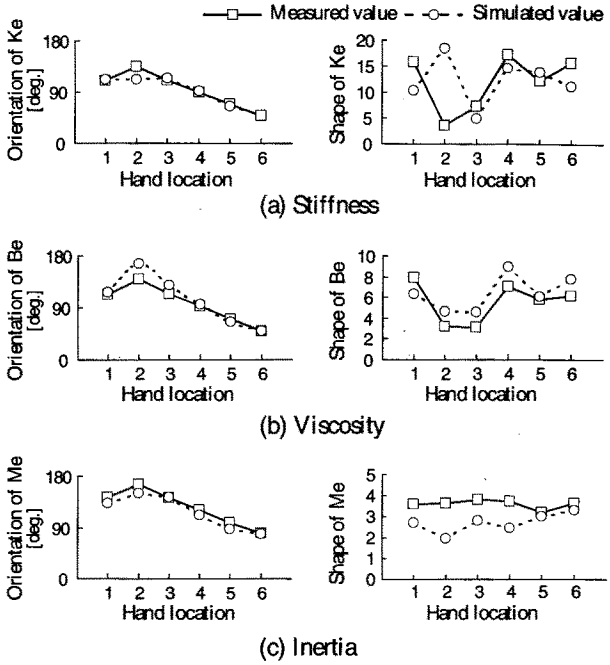

Fig. 5. Geometrical parameters of measured and simulated impedance ellipses of the single arm with changing 2D arm posture for subject B.

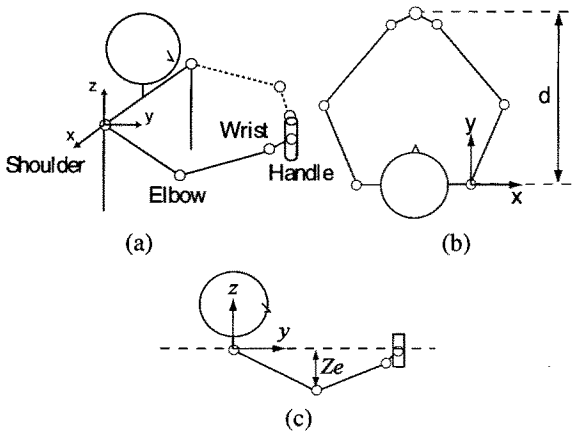

Fig. 6. 3D arm posture.

simulated in six single arm postures using $\boldsymbol{A}_q(\boldsymbol{q})$, which has been modeled by the first and second order polynomial approximations using measured hand impedance on the 61 hand locations for each subject.

Figure 4 shows examples of the simulated impedance, which are compared with the measured ones using the hand impedance ellipses for two subjects, in which the solid line represents the ellipses of the values and the broken line the ellipses of the simulated values.

Figure 5 shows the geometrical parameters of the measured and simulated hand impedance which are the orientation (defined by the counterclockwise angle from the x axis of the task coordinate system to the major axis of the ellipse), and the shape (defined by the ratio between the lengths of the major and minor axes), respectively [3]. As shown in Fig. 5, the simulated hand stiffness and viscosity tend mostly to have similar orientation and shape of the measured stiffness and viscosity ellipses regardless of different hand locations. The simulated hand inertia tends mostly to have a similar shape to that of the measured inertia.

As shown in Fig. 5, except for the hand location number 2, the simulated values agree well with the corresponding measured values. The difference of the length of the stiffness ellipse's minor axis between the simulated and measured value could be caused by the approximation errors of the elbow joint impedance. It is necessary to improve the approximation accuracy, and increase the number of the measured values registered into the database of the *impedance simulator*.

From the above results, it can be seen that the hand impedance in the posture and joint activation levels which has not been measured can be predicted. Then, the simulation of the hand impedance during the single/dual arm movements is attempted by the *impedance simulator* in the following section.

4. EXAMPLE OF SIMULATION RESULTS

4.1. Regulation of the hand impedance characteristics for single arm movements

The hand impedance in several locations and several joint activation levels were simulated using the *impedance simulator*. Here, the joint impedance matrices $\boldsymbol{A}_q(\boldsymbol{q})$ have been modeled from the measured hand impedance at 61 hand locations [3]–[5]. The right arm posture are shown in Fig. 6, and changed the distance d from the subject's body to the hand and the distance Z_e from $x-y$ plane of work space to the elbow joint are changed.

Figures 7 and 8 show the results of the simulated hand impedance by the right arm. These figures represent the stiffness, viscosity ellipses with $d = 0.20 \sim 0.45$ [m] by 0.05 [m], and $Z_e = 0.0, 0.10$ [m] under $d = 0.40$ [m]. As shown in Figs. 7 and 8, our simulated hand impedance ellipses can be characterized as follows: (1) the major axes of the stiffness and viscosity ellipses tend to be oriented toward the shoulder of the subject; (2) the orientation of the major axes of the hand stiffness and viscosity ellipses tends to be rotated counterclockwise as the hand location approaches the subject's body; (3) the ellipses become more elongated as the hand location approaches the distal boundary of the work space; (4) the orientation of the major axes of the hand stiffness ellipses tends to be rotated clockwise, and one of the viscosity ellipses tends to be rotated counterclockwise as the elbow position lowers from $x-y$ plane of work space.

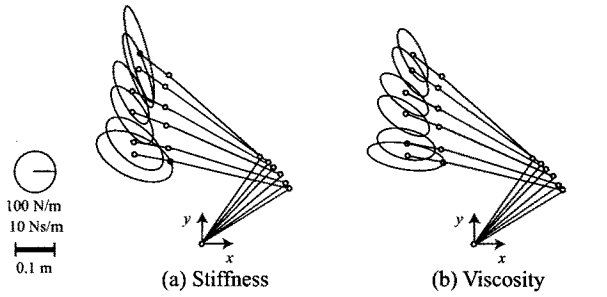

Fig. 7. Simulated impedance ellipses by the single arm according to the hand position d under the elbow position Z_e = 0.0 [m].

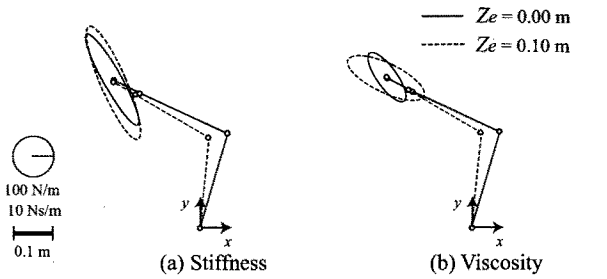

Fig. 8. Simulated impedance ellipses by the single arm according to the elbow position Z_e under the hand position d = 0.40 [m].

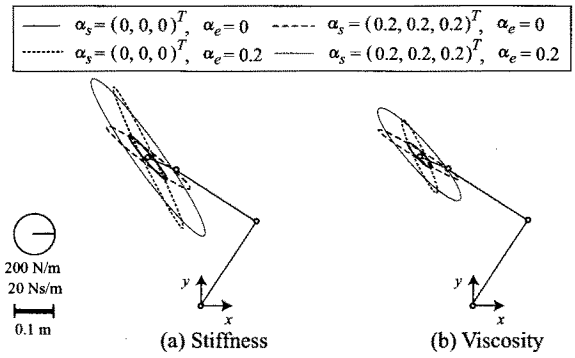

Fig. 9. Simulated impedance ellipses by the single arm with various muscle activation levels under the hand position d = 0.40 [m] and the elbow position Z_e = 0.0 [m].

4.2. Regulation of the hand impedance by changing the joint activation levels

Figure 9 shows the results of the simulated hand impedance by the single arm with various joint activation levels. This figure represents the stiffness and viscosity ellipses by the single arm posture by changing the shoulder and elbow joint activation levels $\boldsymbol{\alpha}_s$,$\boldsymbol{\alpha}_e$ to 0, 20 %. It can be characterized from the results in Fig. 9 that: (1) the orientation of the major axes of the hand stiffness and viscosity ellipses tends to be rotated clockwise as the elbow joint activation levels increase; (2) the major axes of stiffness and viscosity ellipses tend to elongate as the shoulder joint activation levels increase; (3) the area of ellipses increases with respect to the shoulder and elbow joint activation levels.

It can be seen from the above results that: (1) the area of stiffness and viscosity ellipses increase according to the increase of joint activation levels; and (2) the length of the major axes of stiffness and viscosity ellipses can be regulated; but it is difficult to regulate the length of the minor axes of the stiffness and viscosity ellipses. Thus, the hand impedance with various postures and joint activation levels can be predicted without measuring the hand impedance in experiments.

4.3. Regulation of the hand impedance characteristics for dual arm movements

Finally, the hand impedance by the dual arms are the joint impedance matrices $\boldsymbol{A}_q(\boldsymbol{q})$ that had been modeled from the measured hand impedance at 61 hand locations [3]–[5], where the right arm and the left arm have assumed the same impedance characteristics. The dual arm posture of the subjects are shown in Fig. 6, and changed the distance d from the subject's body to the hand are changed where the subjects had a handle in the right and left hands.

Figure 10 shows the results of the simulated hand impedance by the dual arm. This figure represents the stiffness, viscosity and inertia ellipses by the right arm with $d = 0.40, 0.47$ [m]. As shown in the simulated results of each ellipses, it can be found that the orientation of the stiffness and viscosity ellipses almost agree with the y axis of work space, and the orientation of the inertia ellipses almost agree with the x axis of work space. Also, the major axes of stiffness and viscosity ellipses tend to elongate as the distance d from the subject's body to hand increases.

The hand impedance characteristics by the dual arms

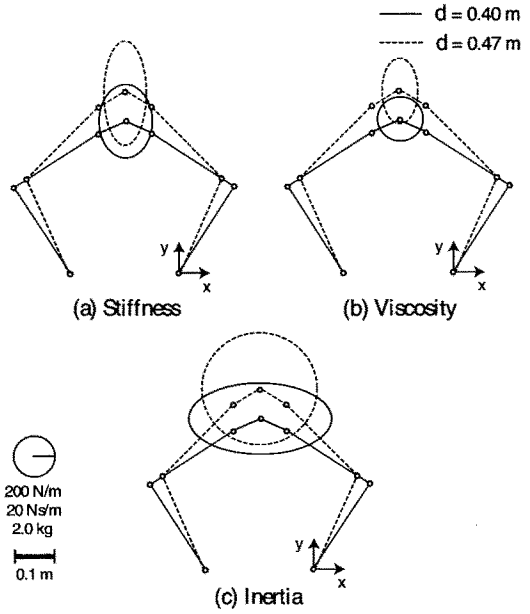

Fig. 10. Simulated hand impedance ellipses by the dual arm according to the hand position d under the elbow position Z_e = 0.0 [m].

almost agree with the characteristics of the experimental results [12]. It can be seen that the hand impedance characteristics with changes of the dual arm posture can almost be approximated using the the hand impedance parameters of the single arm.

5. CONCLUSION

This paper has developed the *impedance simulator* which computes the hand impedance according to changes of the posture and joint activation levels. The following primary points of the *impedance simulator* were found;

1) The developed simulator can predict the hand impedance characteristics during the single arm movements qualitatively.
2) The developed simulator can predict the hand impedance characteristics qualitatively with changes of the dual arm posture using the measured hand impedance parameters by the single arm.

In this paper, only the hand impedance with changes of the arm posture and joint activation levels were simulated. However, the mechanical impedance characteristics of upper extremities is dependent on the change of viscoelasticity by the combination of the contraction level of uniarticalar muscles and biarticalar muscles, and the dynamic changes of hand force. The results of this paper should be extended to the simulation with these characteristics taken into consideration. Also, future research will be performed quantitatively evaluating and computing the hand impedance in three-dimensional postures with the changes of muscle activation levels.

Since the measurement of the EMG signals and joint angle gets gradually easier and can be measured without barring subjects' movements, the hand impedance may be predicted under some working conditions and environments of measurement if the *impedance simulator* can be completed. Also, the *impedance simulator* can be useful, not only for the human movement analysis, but the development of robot and welfare apparatuses.

ACKNOWLEDGMENT

This research was supported by Grant-in-Aid for Scientific Research of Japan Society for the Promotion of Science (15008210) and The Ministry of Education, Culture, Sports, Science and Technology (14750188 and 15360226).

REFERENCES

[1] F.A.Mussa-Ivaldi, N.Hogan and E.Bizzi : Neural, mechanical and geometric factors subserving arm in humans, Journal of Neuroscience, Vol.5, No.10, 2732/2743 (1985).
[2] J.M.Dolan, M.B.Friendman and M.L.Nagarka : Dynamics and loaded impedance components in the maintenance of human arm posture, IEEE Transaction on Systems, Man and Cybernetics, Vol.23, 3, 698/709 (1993).
[3] T.Tsuji, P.Morasso, K.Goto and K.Ito : Human Hand Impedance Characteristics during Maintained Posture in Multi-Joint Arm Movements, Biological Cybernetics, Vol.72, 475/485 (1995).
[4] T. Tsuji, M. Moritani, M. Kaneko and K. Ito : An Analysis of Human Hand Impedance Characteristics during Isometric Muscle Contractions, Transactions of the Society of Instrument and Control Engineers, Vol. 32, No. 2, 271/289, (1996) (in Japanese).
[5] T. Tsuji and M. Kaneko : Estimation and Modeling of Human Hand Impedance during Isometric Muscle Contraction, Proceedings of the ASME Dynamic Systems and Control Division, DSC-Vol. 58, 575/582 (1996).
[6] R. Osu, and H. Gomi : Multijoint Muscle Regulation Mechanisms Examined by Measured Human Arm Stiffness and EMG signals, Journal of Neurophysiology, Vol. 81, No. 4, 1458/1468 (1999).
[7] H. Gomi and M. Kawato : Equilibrium-Point Control Hypothesis Examined by Measured Arm Stiffness During Multijoint Movement, SCIENCE, Vol. 272, 117/120 (1996).
[8] T.Flash : The Control of Hand Equilibrium Trajectories in Multi-Joint Arm Movements, Biological Cybernetics, Vol.57, 257/274 (1987).
[9] M.Katayama and M. Kawato : Virtual trajectory and stiffness ellipse during multijoint arm movement predicted by neural inverse model, Biological Cybernetics, Vol.69, 353/362 (1993).
[10] T.Flash and I.Gurevich : Model of moter adaptation and impedance control in human arm movements, Self-Organization, Computional Maps, and Motor Control, 423/481 (1997).
[11] P.L.Weiss, R.E.Kearney and I.W.Hunter : Position Dependence of Ankle Joint Dynamics - I. Passive Mechanics, Journal of Biomechanics, Vol.19, No.9, 727/735 (1986).
[12] Y.Takeda, T.Tsuji : Human Impedance Characteristics During the Dual Arm Movements, Proceedings of the Conference of the Society of Biomechanisms in Japan, 43/46 (2002) (in Japanese).
[13] P.L.Weiss, I.W.Hunter and R.E.Kearney : Human Ankle Joint Stiffness Over the Full Range of Muscle Activation Levels, Journal of Biomechanics, Vol.21, No.7, 539/544 (1988).

Author:
IMPEDANCE SIMULATOR: ANALYSIS OF HUMAN HAND IMPEDANCE CHARACTERISTICS,
Y.Takeda, Y. Tanaka, and T. Tsuji are with Department of Artificial Complex Systems Engineering, Hiroshima University , 1-4-1 Kagamiyama, Higashi-Hiroshima, Hiroshima, 739-8527 Japan.
Phone: +81 824 24 7676, Fax: +81 824 22 7030
E-mail: takeda@bsys.hiroshima-u.ac.jp,
ytanaka@bsys.hiroshima-u.ac.jp,
tsuji@bsys.hiroshima-u.ac.jp